



# Modulational instabilities of periodic traveling waves in deep water



Benjamin F. Akers

Department of Mathematics and Statistics, Air Force Institute of Technology, Dayton, OH, United States

## HIGHLIGHTS

- The spectrum of traveling water waves is asymptotically approximated, considering two and three-dimensional perturbations.
- A multiple scale expansion is employed, coupling wave slope to Bloch parameter.
- The radius of the disc of analyticity of the spectrum is predicted, and compared to numerical simulations.
- Modulational instabilities are computed.

## ARTICLE INFO

### Article history:

Received 12 August 2014  
 Received in revised form  
 19 December 2014  
 Accepted 18 February 2015  
 Available online 5 March 2015  
 Communicated by J. Bronski

### Keywords:

Stability  
 Water waves  
 Resonance  
 Benjamin–Feir

## ABSTRACT

The spectrum of periodic traveling waves in deep water is discussed. A multi-scale method is used, expanding the spectral data and the Bloch parameter in wave amplitude, to compute the size and location of modulated instabilities. The role of these instabilities in limiting the spectrum's analyticity is explained. Both two-dimensional and three-dimensional instabilities are calculated. The asymptotic predictions are compared to numerical simulations.

Published by Elsevier B.V.

## 1. Introduction

The spectral stability of traveling deep-water waves is studied. The water wave stability problem has a rich history, with great strides made in the late sixties with the work of Benjamin and Feir [1] and the development of Resonant Interaction Theory (RIT) [2–5]. The predictions of RIT have since been leveraged heavily by numerical methods; the influential works of MacKay and Saffman [6] and McLean [7] led to a taxonomy of water wave instabilities based on RIT. The most recent review article is that of Dias and Kharif [8]; since the publication of this review a number of modern numerical stability studies have been conducted [9–13].

In RIT, wave dynamics are studied using approximate models for the evolution of the amplitude of a small number of weakly nonlinear wave modes: triads, quartets, etc. Examples of such model equations which include modulational effects are the nonlinear Schrödinger equation, the Dysthe equation, and the Davey–Stewartson/Benney–Roskes equations [4,14–16]. The stability of Stokes waves has been studied in such models, often they were derived for exactly this purpose [17–19].

In this work, the spectrum of traveling water waves is approximated via small amplitude asymptotic expansion. This approach contrasts the vast majority of spectral stability computations, which are primarily numerical. Typical numerical computations calculate the spectrum via an eigensolver at each fixed amplitude—see for example [9,20,10]. Boundary perturbation methods take an alternative approach, expanding the traveling wave and spectrum in amplitude. Boundary perturbation methods calculate the coefficients of a series representation of the spectrum. Boundary perturbation methods have been applied to compute water waves numerous times [21–24] and are reviewed in [25]. This approach is employed for the water wave spectrum in [26,27].

In a series of recent works, the author and collaborators derived the weakly nonlinear asymptotics of the spectrum in conjunction with the development of boundary perturbation methods, for deep water gravity waves in [13], including surface tension in [28], and with finite depth effects in [29]. Each article in this series considers a two-dimensional fluid, and expands the spectrum in amplitude at a sampling of fixed Bloch parameters; instabilities which have both fixed Bloch parameter and are analytic in amplitude are observed to be rare.

It is known that small amplitude instabilities bifurcate from a set of resonant configurations, whose locations may be predicted

E-mail address: [Benjamin.Akers@afit.edu](mailto:Benjamin.Akers@afit.edu).

by linear theory [7,8]. These resonant configurations are the Bloch parameters for which the spectrum of the linearization about the flat-state contains eigenvalue collisions. It is known that the spectrum is analytic as a function of amplitude at all Bloch parameters where the flat-state eigenvalues are simple [30]. Recent numerical simulations suggest that the spectrum is also analytic at eigenvalue collisions, but that the radius of the disc of analyticity vanishes as the Bloch parameter approaches the resonant configurations [28,29]. This vanishing radius has been proposed as a mechanism for detecting instabilities [27].

The potential flow equations have traveling wave solutions which are analytic in wave slope [31]. The leading asymptotics of the traveling wave have been computed numerous times [32–35]. The asymptotics of the spectrum have been computed for a two-dimensional fluid in [13,28,29], these asymptotics all compute the spectrum with fixed Bloch parameter. In this work, instabilities are computed with Bloch parameters which depend on amplitude, on both a two-dimensional and three-dimensional fluid. We use a multi-scale expansion which couples frequency and amplitude in a manner analogous to the modulational ansatz which is typically used to derive envelope equations [14,36,16]; we refer to the unstable spectral data computed in this manner as modulational instabilities.

Often the term modulational is used to refer only to the Benjamin–Feir instability. Although much of the asymptotic work regarding Benjamin–Feir dates back to the 1960s and RIT, more recently a number of authors have been pursuing rigorous proof of the existence of this instability in a variety of wave models [37,38]. Most similar in spirit to this work is that in [39,40], where an analogous perturbation in Bloch parameter is used. Although we consider only formal asymptotics, such asymptotics have been used as the basis for proofs of the existence of solutions in the TFE framework [31,30].

In the current framework, the classic long wave modulational instability, Benjamin–Feir, is recovered as are many other modulational instabilities. The onset of instability at fixed Bloch parameter, and thus the amplitude at which the fixed Bloch parameter spectrum loses analyticity, is predicted. Both two-dimensional and three-dimensional perturbations are considered. The asymptotic instability locations are compared with the numerical estimates of these locations using the method of Akers and Nicholls [13,28].

The paper is organized as follows. Section 2 begins by introducing the spectral stability problem for water waves. The asymptotics of the spectrum are then presented, in subsections organized by the type of resonance which is responsible for the flat-state eigenvalue collisions. Triad resonance is presented in Section 2.1; quartets are discussed in Section 2.2. We comment on higher order resonances in 2.3, and finally compute the Benjamin–Feir instability in Section 2.4.

## 2. Modulational instabilities of deep water waves

The widely-accepted model for irrotational motions of a large body of deep water in the absence of viscosity is the Euler equations

$$\phi_{xx} + \phi_{yy} + \phi_{zz} = 0, \quad z < \epsilon\eta, \quad (2.1a)$$

$$\phi_z = 0, \quad z \rightarrow -\infty, \quad (2.1b)$$

$$\eta_t + \epsilon(\eta_x\phi_x + \eta_y\phi_y) = \phi_z, \quad z = \epsilon\eta, \quad (2.1c)$$

$$\phi_t + \frac{\epsilon}{2}(\phi_x^2 + \phi_y^2 + \phi_z^2) + \eta - \sigma \left( \frac{\eta_{xx} + \eta_{yy}}{(1 + \epsilon^2(\eta_x^2 + \eta_y^2))^{3/2}} \right) = 0, \quad z = \epsilon\eta, \quad (2.1d)$$

where  $\eta$  is the free-surface displacement and  $\phi$  is the velocity potential. System (2.1) has been nondimensionalized as in [13,41].

We assume that the wave slope,  $\epsilon = A/L$  is small ( $A$  is a typical displacement and  $L$ , the characteristic horizontal length, is chosen so that waves in (2.1) have spatial period  $2\pi$ ). The constant  $\sigma = \frac{\gamma}{g L^2}$  is a Bond number comparing the relative importance of gravity,  $g$ , to surface tension  $\gamma$ .

The potential flow equations (2.1), have traveling wave solutions which depend analytically on wave slope [31]. These solutions can be written in terms of the speed  $c$ , the displacement  $\eta$ , and the free surface trace of the potential  $\Phi$ , each as a series in  $\epsilon$ . Periodic traveling wave solutions are often called Stokes' waves, as the leading order terms of this series were first written by Stokes [32]. We consider the stability of the classic Stokes wave, which is constant in transverse direction, and at leading order is supported at wavenumber  $k_0 = (1, 0)$ . The speed, displacement and free surface trace of the potential of this wave are, to  $O(\epsilon^2)$ ,

$$c = \sum_{n=0}^{\infty} \epsilon^n c_n = \begin{pmatrix} \sqrt{1+\sigma} \\ 0 \end{pmatrix} + \epsilon^2 \begin{pmatrix} 2\sigma^2 + \sigma + 8 \\ 4(1-2\sigma)\sqrt{1+\sigma} \end{pmatrix} + O(\epsilon^3), \quad (2.2a)$$

$$\bar{\eta} = \sum_{n=1}^{\infty} \epsilon^n \bar{\eta}_n = \epsilon e^{ik_0 \cdot \mathbf{x}} + \epsilon^2 \left( \frac{1+\sigma}{1-2\sigma} \right) e^{2ik_0 \cdot \mathbf{x}} + * + O(\epsilon^3), \quad (2.2b)$$

$$\bar{\Phi} = \sum_{n=1}^{\infty} \epsilon^n \bar{\Phi}_n = \epsilon i \sqrt{1+\sigma} e^{ik_0 \cdot \mathbf{x}} + \epsilon^2 \begin{pmatrix} 3i\sigma\sqrt{1+\sigma} \\ 1-2\sigma \end{pmatrix} e^{2ik_0 \cdot \mathbf{x}} + * + O(\epsilon^3). \quad (2.2c)$$

In (2.2), the  $*$  refers to the complex conjugate of the preceding terms. This traveling wave solution is constant in the transverse horizontal direction, here  $y$ . Later the perturbations of this wave will be permitted to have non-trivial dependence on both horizontal coordinates,  $\mathbf{x} = (x, y)$ .

The spectral stability of these traveling waves (2.2) is considered by writing Eq. (2.1) in terms of the free surface trace  $\Phi$  and displacement  $\eta$ , as in [42], then substituting the ansatz

$$\begin{aligned} \eta &= \bar{\eta}(\mathbf{x} + ct) + \delta\zeta(\mathbf{x} + ct)e^{\lambda t}, \quad \text{and} \\ \Phi &= \bar{\Phi}(\mathbf{x} + ct) + \delta u(\mathbf{x} + ct)e^{\lambda t}, \end{aligned} \quad (2.3)$$

and neglecting quadratic powers of  $\delta$ . The result is a generalized spectral problem of the form

$$A(\bar{\eta}, \bar{\Phi}, c)w = \lambda B(\bar{\eta}, \bar{\Phi}, c)w, \quad (2.4)$$

where  $w = (\zeta, u)^T$ . Traveling waves are considered spectrally unstable if solutions to (2.4) have  $\lambda$  with positive real part. It is straightforward to calculate the operators  $A$  and  $B$ , and we refer the interested reader to [13,28].

To solve (2.4), we must append boundary conditions for  $w$ . Rather than assuming perturbations  $w$  share a period with the traveling waves, thus restricting to superharmonic perturbations [43], we consider arbitrary periods, including subharmonic perturbations [44]. Subharmonic perturbations satisfy Bloch (quasi) periodic boundary conditions [45]. If the traveling wave is  $x$ -periodic with period  $L$ , then the perturbations satisfy

$$w(x + L, y) = e^{ipL}w(x, y). \quad (2.5)$$

For  $L = 2\pi$ -periodic traveling waves, it is sufficient to consider the set of Bloch parameters with  $p \in [0, 1)$ . Similar conditions apply in the  $y$ -direction, whose corresponding Bloch parameter is labeled  $q$ ; we will combine these two parameters in a vector  $\kappa = (p, q)^T$ .

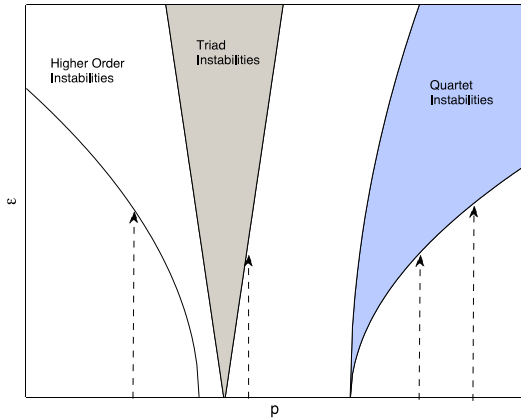


**Fig. 2.1.** A cartoon depicts the location of two-dimensional instabilities in the Bloch parameter–amplitude plane. As derived in the following sections, triad instabilities have linear boundaries,  $p - p_0 = O(\epsilon)$ . Quartet instabilities have square root boundaries,  $p - p_0 = O(\epsilon^2)$ . Higher order instabilities occur near curves which have the quartet boundary scaling, but have asymptotically small,  $O(\epsilon^r)$  with  $r > 2$ , width. All of these instabilities would cause a fixed Bloch parameter boundary perturbation method to lose analyticity. The dashed arrows depict trajectories along which a non-modulational method, like that of [28], would be able to compute the spectrum.

Solutions to the spectral stability problem, Eq. (2.4), can also be written as a series in amplitude, see [30,27],

$$\zeta(x, y) = \sum_{n=0}^{\infty} \epsilon^n \zeta_n(x, y),$$

$$u(x, y) = \sum_{n=0}^{\infty} \epsilon^n u_n(x, y), \quad \lambda = \sum_{n=0}^{\infty} \epsilon^n \lambda_n. \quad (2.6)$$

The main thrust of this paper is the role that the boundary conditions play in the analyticity of the spectral data,  $\lambda$ ,  $\zeta$  and  $u$ , as functions of wave slope  $\epsilon$ . For a two-dimensional fluid, with fixed Bloch parameter,  $p$ , the corrections  $\lambda_n$ ,  $\zeta_n$  and  $u_n$  have been computed about simple eigenvalues in [30] and about repeated eigenvalues in [13,28]. Because the form of these series (2.6) changes at repeated eigenvalues, the radius of convergence is typically discontinuous in the neighborhood of resonant Bloch parameters (those with flat-state eigenvalue collisions). Often the spectrum has finite disc of analyticity at a resonant Bloch parameter, but will have a vanishingly small disc of analyticity as the Bloch parameter approaches this configuration. Such discontinuities in radii are reported in [28,29]. This dependence of the disc of analyticity is explained here by locating the curves in the Bloch parameter amplitude plane where finite amplitude instabilities occur; these instabilities necessarily cause the spectrum to lose analyticity. A cartoon of the instability locations is presented in Fig. 2.1.

In the following sections, the instabilities which limit the spectrum's analyticity will be described using an asymptotic expansion which couples amplitude and Bloch vector,

$$\kappa = \kappa_0 + \epsilon \kappa_1 + \epsilon^2 \kappa_2 + \dots,$$

where each correction to the Bloch vector is labeled  $\kappa_j = (p_j, q_j)^T$ . To begin, we consider the flat-state,  $\epsilon = 0$ , problem. It is a simple calculation to recover the spectrum of infinitesimal waves

$$\lambda_0 = \pm i\omega(k_j) + ic_0 \cdot k_j, \quad (2.7)$$

where  $\omega(k) = \pm \sqrt{|k|(1 + \sigma|k|^2)}$  and for planar Stokes waves  $c_0 = (\sqrt{1 + \sigma}, 0)^T$ . With Bloch boundary conditions, the wave numbers are expressed as  $k_j = (m_j, n_j)^T + (p_0, q_0)^T$ , with  $m_j, n_j \in \mathbb{Z}$  and  $p_0, q_0 \in [-1, 1)$ . A flat-state eigenvalue collision,  $\lambda_0(k_1) = \lambda_0(k_2)$ , implies a resonance condition between the temporal frequencies

$$\pm \omega(k_1) \mp \omega(k_2) = c_0 \cdot (k_1 - k_2) = (m_1 - m_2)\omega(k_0). \quad (2.8)$$

Eq. (2.8) is fundamental in understanding instabilities of Stokes waves. Examining the left and rightmost sides of (2.8), flat-state eigenvalue collisions occur when the wave numbers of the perturbations,  $k_1$  and  $k_2$  resonate with  $\Delta m = m_1 - m_2$  copies of the Stokes wave, at frequency  $k_0$ . It is the resonant mixing of these wave numbers that may lead to instabilities; only near these resonances may finite amplitude eigenvalue collisions and instabilities occur [7,8]. The difference between the first component of the wavenumbers of the perturbations,  $\Delta m$ , determines the type of resonance, and the character of the spectrum. For this reason it is natural to present the results in using the naming conventions of Resonant Interaction Theory [3]. When this difference is  $\Delta m_j = 1$  the eigenvalue collision is due to a triad resonance. Similarly  $\Delta m = 2$  is a quartet resonance,  $\Delta m = 3$  is a quintet, etc. Although collisions of more than two eigenvalues are rare, we include the asymptotics of the spectrum about one collision of four flat-state eigenvalues, the Benjamin–Feir case.

The same base perturbation series can be used to derive the leading eigenvalue correction in all cases, by beginning with a leading order perturbation of the form

$$\begin{pmatrix} \zeta_0 \\ u_0 \end{pmatrix} = \beta_{0,1} \begin{pmatrix} 1 \\ \lambda_0 + ic_0 \cdot k_1 \\ |k_1| \end{pmatrix} e^{ik_1 \cdot x} \\ + \beta_{0,2} \begin{pmatrix} 1 \\ \lambda_0 + ic_0 \cdot k_2 \\ |k_2| \end{pmatrix} e^{ik_2 \cdot x} + \beta_{0,3} \begin{pmatrix} 0 \\ 1 \end{pmatrix}. \quad (2.9)$$

We will normalize the eigenfunctions so that  $\beta_{0,1} = 1$ . When the flat-state eigenvalue,  $\lambda_0$ , has algebraic multiplicity of two,  $\beta_{0,3}$  will be set to zero; to consider the Benjamin–Feir case the wave numbers of the perturbations are set as  $k_1 = k_0$ , and  $k_2 = -k_0$ . The  $O(\epsilon)$  corrections to the perturbation solve a forced linear partial differential equation,

$$\begin{pmatrix} \lambda_0 + c_0 \partial_x & \mathcal{L} \\ 1 - \sigma \Delta & \lambda_0 + c_0 \partial_x \end{pmatrix} \begin{pmatrix} \zeta_1 \\ u_1 \end{pmatrix} \\ + \sum_{j=1}^3 \sum_{m=-1}^1 \beta_{0,j} \begin{pmatrix} q_j^m \\ Q_j^m \end{pmatrix} e^{i(k_j + mk_0) \cdot x} = 0, \quad (2.10)$$

where  $\mathcal{L}$  is the operator induced by z-derivatives using a Dirichlet-to-Neumann map, as in [42,46], with Fourier symbol  $\hat{\mathcal{L}}(k) = |k|$ .

The forcing in Eq. (2.10) is introduced in two ways. First, nonlinear interactions between the leading order perturbation  $(\zeta_0, u_0)$  with the leading order Stokes wave  $(\eta_1, \Phi_1)$  generate the coefficients  $q_j^{\pm 1}, Q_j^{\pm 1}$ . Second, the first variation of the linear operators when expanded in Bloch parameter generates the  $q_j^0, Q_j^0$ , which contain the modulational contribution to this series. The nonlinear interaction coefficients were reported for a two dimensional fluid in [28], and are calculated for a three-dimensional fluid below. The coefficients of the forcing terms, for  $j = 1, 2$  are

$$q_j^{\pm 1} = i(k_j \pm k_0) \cdot \left( ik_j \frac{(\lambda_0 + ic_0 \cdot k_j)}{|k_j|} - k_0 \frac{1 + \sigma}{c_0 \cdot k_0} \right),$$

$$Q_j^{\pm 1} = \left( i(1 + \sigma)(\pm |k_j| - k_0 \cdot k_j) \frac{\lambda_0 + ic_0 \cdot k_j}{(c_0 \cdot k_0)|k_j|} \right. \\ \left. - \omega(k_j)^2 - \omega(k_0)^2 \right),$$

$$q_j^0 = \lambda_1 + \left( ic_0 - \frac{\lambda_0 + ic_0 \cdot k_j}{|k_j|^2} k_j \right) \cdot \kappa_1,$$

$$Q_j^0 = \left( \frac{\lambda_0 + ic_0 \cdot k_j}{|k_j|} \right) (\lambda_1 + ic_0 \cdot \kappa_1) + 2\sigma k_j \cdot \kappa_1.$$

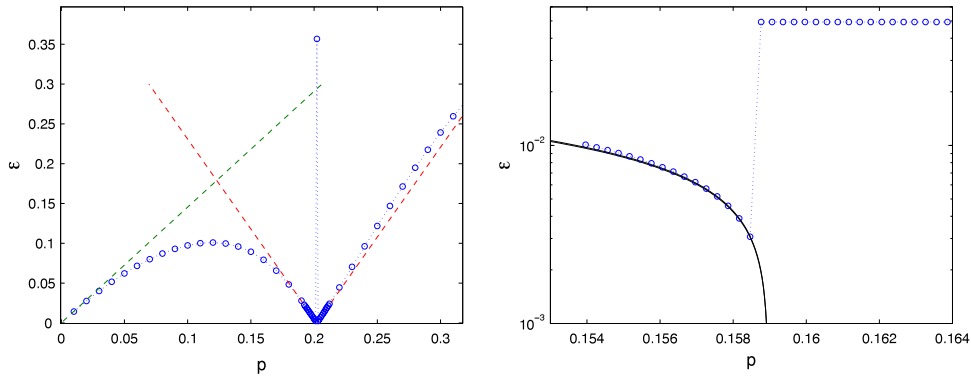


**Fig. 2.2.** Left: The numerical estimates of the radii of convergence,  $\epsilon$ , of a series expansion of the spectrum based on the TFE method of [28] at  $\sigma = 3$ , marked with circles, are compared to the asymptotic prediction of Eq. (2.13), marked with the solid lines emanating from  $p_0 \approx 0.202$ . Notice that circles are not continuous at the resonant Bloch parameter  $p_0 \approx 0.202$ , having a limit of zero but a value of  $\epsilon \approx 0.35$ . The Benjamin–Feir instability is also marked with the solid line emanating from  $p_0 = 0$ , using (2.25). Right: The TFE predictions for the radii of convergence,  $\epsilon$ , of the spectrum near a quartet resonance is depicted as a function of the Bloch parameter  $p$  at  $\sigma = 0.24$ . The predictions of Eq. (2.18) are marked with two solid (almost overlapping) curves.

The eigenfunction at wavenumber  $k_3 = 0$  is treated specially. The forcing terms due to interaction with this wavenumber have  $q_3^{\pm 1} = Q_3^{\pm 1} = 0$  and

$$q_3^0 = -|\kappa_1|,$$

$$Q_3^0 = \lambda_1 + ic_0 \cdot \kappa_1.$$

Eq. (2.10) is always solvable;  $\lambda_1$  is set by enforcing the Fredholm condition, that the forcing terms are orthogonal to  $\Psi_j$  in the kernel of the adjoint of linear operator in (2.10),

$$\begin{pmatrix} (\bar{\lambda}_0 - c_0 \partial_x) & \mathcal{L} \\ 1 - \sigma \Delta & (\bar{\lambda}_0 - c_0 \partial_x) \end{pmatrix} \Psi_j = 0.$$

The  $\Psi_j$  are labeled based on their support, which is at the same wave numbers as the leading order eigenvectors  $(\zeta_0, u_0)$ , at  $k_1, k_2$ , and in the Benjamin–Feir case  $k_3$ .

$$\Psi_j = \begin{pmatrix} 1 \\ -\bar{\lambda}_0 - ic_0 \cdot k_j \\ 1 + \sigma |k_j|^2 \end{pmatrix} e^{ik_j \cdot x}. \quad (2.11)$$

Enforcing solvability, orthogonality of the forcing terms to  $\Psi_j$ , yields different equations for  $\lambda_1$  depending on the difference in frequency between the wave numbers  $k_1, k_2$  and  $k_3$ . In the following sections we discuss the solvability conditions, and their solutions, categorized by this frequency difference.

### 2.1. Triads

In this section the first eigenvalue correction  $\lambda_1$  is computed. The correction is nonzero only when  $k_1 \pm k_0 = k_2$  which we refer to as a triad. If a triad occurs, we label the wavenumbers so that  $k_1 - k_0 = k_2$ . With this labeling, imposing orthogonality of the forcing terms to  $\Psi_1$  and  $\Psi_2$  gives

$$2(\lambda_1 + i(c_0 - c_g(k_1)) \cdot \kappa_1) + \beta_{0,2} \tau_1 = 0, \quad (2.12a)$$

$$2\beta_{0,2}(\lambda_1 + i(c_0 - c_g(k_2)) \cdot \kappa_1) + \tau_2 = 0, \quad (2.12b)$$

where

$$\tau_1 = q_2^{-1} - \left( \frac{\lambda_0 + ic_0 \cdot k_1}{1 + \sigma |k_1|^2} \right) Q_2^{-1}, \quad \text{and}$$

$$\tau_2 = q_1^+ - \left( \frac{\lambda_0 + ic_0 \cdot k_2}{1 + \sigma |k_2|^2} \right) Q_1^{+1}.$$

For a general triad, the  $\tau_j \neq 0$ , and the first nonzero correction to the flat-state spectrum is

$$\lambda_1 = -i \left( c_0 - \frac{c_g(k_1) + c_g(k_2)}{2} \right) \cdot \kappa_1 \pm \frac{1}{2} \sqrt{\tau_1 \tau_2 - ((c_g(k_2) - c_g(k_1)) \cdot \kappa_1)^2},$$

where  $c_g(k_j) = \omega_k(k_j)$  is the group velocity vector at frequency  $k_j$ .

Both  $\tau_j$  are pure imaginary, so if  $\tau_1 \tau_2 > 0$ , then there is a band of  $\kappa_1$  where instabilities occur, which includes the non-modulated case  $\kappa_1 = 0$ . If  $\kappa_1$  is parallel to the difference of the group velocities, i.e. longitudinal perturbations, then instabilities exist within the interval

$$|\kappa_1| < \frac{\sqrt{\tau_1 \tau_2}}{|c_g[k_1] - c_g[k_2]|}. \quad (2.13)$$

The largest triad instabilities are the non-modulational ones; the triads in the band of instabilities where  $\lambda_1$  has the largest real part are at  $\kappa_1 = 0$ .

Eq. (2.13) predicts the location of finite amplitude instabilities near triads on both two and three-dimensional fluids. It also predicts the vanishing radius of convergence of a fixed Bloch parameter boundary perturbation scheme in the neighborhood of a triad resonance. In the left panel of Fig. 2.2, estimates of the radius of convergence of the TFE method of Akers and Nicholls, computed by the first non-canceled pole of a Padé' interpolant, is compared to the prediction of Eq. (2.13), with good agreement.

### 2.2. Quartets

If the wave numbers of the eigenvalue in question do not participate in a triad interaction, then the  $\tau_j$  are absent in (2.12), and the first eigenvalue correction is pure imaginary

$$\lambda_1 = i(c_g(k_1) - c_0) \cdot \kappa_1.$$

This is the case at quartets. For a typical quartet interaction, where  $c_g(k_1) \neq c_g(k_2)$ , Eqs. (2.12) imply  $\beta_{0,2} = 0$ . For quartets with nonzero  $\lambda_1$  and  $\beta_{0,2} = 0$ , the spectrum behaves like a stable triad, and there is no instability. To compute modulated quartet instabilities,  $\beta_{0,2}$  must be undetermined at this order, which occurs when

$$c_g(k_1) \cdot \kappa_1 = c_g(k_2) \cdot \kappa_1.$$

This condition is satisfied at generic wave numbers  $k_j$  if  $\kappa_1 = 0$ , so that  $\lambda_1 = 0$ , and the leading correction to the flat-state spectrum is  $\lambda_2$ . Note, as presented in Section 2.4, the Benjamin–Feir instability

is a special quartet, where the wave numbers also take part in a degenerate triad interaction (one where the above group velocity condition is satisfied). The Benjamin–Feir instability is of quartet type, but with non-zero  $\lambda_1$ .

After computing  $\lambda_1$ , Eq. (2.10) is solvable, with solution

$$\begin{pmatrix} \zeta_1 \\ u_1 \end{pmatrix} = \sum_{j=1,2} \sum_{m=-1}^1 \beta_{0,j} \begin{pmatrix} \gamma_j^m \\ \Gamma_j^m \end{pmatrix} e^{i(k_j+m k_0) \cdot \mathbf{x}} + \begin{pmatrix} \zeta_{1,h} \\ u_{1,h} \end{pmatrix}. \quad (2.14)$$

The  $u_{1,h}$  and  $\zeta_{1,h}$  are homogeneous solutions of (2.10), which do not effect the stability results presented herein. When computing the eigenvalue corrections to all orders in wave slope, one should choose the homogeneous solutions to have zero support at  $k_1$ , as in [13]. The size of the homogeneous solutions is determined by solvability at later orders. The coefficients in (2.14) have been explicitly calculated,

$$\gamma_j^{\pm 1} = -\frac{(\lambda_0 + i c_0 \cdot (k_j \pm k_0)) q_j^{\pm 1} + |k_j \pm k_0| Q_j^{\pm 1}}{(\lambda_0 + i c_0 \cdot (k_j \pm k_0))^2 + (1 + \sigma |k_j \pm k_0|^2) |k_j \pm k_0|}, \quad (2.15a)$$

$$\gamma_j^0 = -\frac{q_j^0}{2(\lambda_0 + i c_0 \cdot k_j)}, \quad (2.15b)$$

$$\Gamma_j^{\pm 1} = -\frac{(\lambda_0 + i c_0 \cdot (k_j \pm k_0)) Q_j^{\pm 1} - (1 + \sigma |k_j \pm k_0|^2) q_j^{\pm 1}}{(\lambda_0 + i c_0 \cdot (k_j \pm k_0))^2 + (1 + \sigma |k_j \pm k_0|^2) |k_j \pm k_0|}, \quad (2.15c)$$

$$\Gamma_j^0 = \frac{-Q_j^0}{2(\lambda_0 + i c_0 \cdot k_j)}. \quad (2.15d)$$

The equation for the next corrections ( $\zeta_2$ ,  $\eta_2$ ) and  $\lambda_2$  is

$$\begin{pmatrix} \lambda_0 + c_0 \partial_x & \mathcal{L} \\ 1 - \sigma \Delta & \lambda_0 + c_0 \partial_x \end{pmatrix} \begin{pmatrix} \zeta_2 \\ u_2 \end{pmatrix} + \sum_{j=1}^2 \sum_{m=-2,0,2} \beta_{0,j} \begin{pmatrix} t_j^m \\ T_j^m \end{pmatrix} e^{i(k_j+m k_0) \cdot \mathbf{x}} = 0. \quad (2.16)$$

The coefficients  $t_j^m$  and  $T_j^m$  are due to interactions of wavenumber  $k_j$  with the Stokes wave  $k_0$  in the nonlinear terms of (2.1) as well as the second variation of the linear operators with respect to Bloch parameter. They are analogous to the  $q_j^m$  in Eq. (2.10), excepting that the terms  $t_j^0$  and  $T_j^0$  include both the nonlinear interaction and the expansion of the linear operators (where as  $q_j^0$  and  $Q_j^0$  include only contributions from the expansion of the linear operator, without any contributions from the nonlinearity). The coefficients are reported below as  $t_j^0 = (t_j^0)_L + (t_j^0)_N$  and  $T_j^0 = (T_j^0)_L + (T_j^0)_N$  to emphasize the different origins. As with the previous section, the nonlinear contributions were computed for two-dimensional fluids absent modulation in [13]. The modulational and three-dimensional coefficients extension was calculated here using the results of [13]. It is worth noting that the effect of modulation was calculated to quintic order in the context of the Zakharov equation by Stiassnie and Shemer [17], in which the below coefficients are also calculated.

$$\begin{aligned} (t_j^0)_L &= \lambda_2 + i c_0 \cdot \kappa_2 + i c_2 \cdot k_j - \left( \frac{1}{2} \kappa_1^T \hat{\mathcal{L}}_{kk}(k_j) \kappa_1 + \hat{\mathcal{L}}_k(k_j) \cdot \kappa_2 \right) \\ &\quad \times \frac{i \omega(k_j)}{|k_j|} + (\lambda_1 + i c_0 \cdot \kappa_1) \gamma_j^0 - \hat{\mathcal{L}}_k(k_j) \cdot \kappa_1 \Gamma_j^0, \end{aligned}$$

$$\begin{aligned} (t_j^0)_N &= i k_j \cdot (i(k_j + k_0) \Gamma_j^{+1} + i(k_j - k_0) \Gamma_j^{-1} \\ &\quad - k_0(c_0 \cdot k_0)(\gamma_j^{+1} + \gamma_j^{-1}) - 2k_0(c_0 \cdot k_0) - k_j \omega(k_j)), \end{aligned}$$

$$\begin{aligned} t_j^{\pm 2} &= i(k_2 \pm 2k_0) \cdot \left( i(k_j \pm k_0) \Gamma_j^{\pm 1} - k_0(c_0 \cdot k_0) \gamma_j^{\pm 1} \right. \\ &\quad \left. + 2i k_0 F_2 - E_2 \frac{\omega(k_j)}{|k_j|} k_j - k_0(c_0 \cdot k_0) - \frac{1}{2} \omega(k_j) k_j \right). \end{aligned}$$

The symbol  $\hat{\mathcal{L}}(k_j) = |k_j|$  is the Fourier transform of the operator induced by  $z$ -derivatives, using the Dirichlet-to-Neumann map, as in [42]. The symbols  $\hat{\mathcal{L}}_k(k_j)$  and  $\hat{\mathcal{L}}_{kk}(k_j)$  are its gradient and Hessian respectively.

$$\begin{aligned} (T_j^0)_L &= (\lambda_2 + i c_0 \cdot \kappa_2 + i c_2 \cdot k_j) \frac{\lambda_0 + i c_0 \cdot k_j}{|k_j|} + (\sigma |\kappa_1|^2 \\ &\quad + 2\sigma k_j \cdot \kappa_2) + (\lambda_1 + i c_0 \cdot \kappa_1) \Gamma_j^0 + 2\sigma k_j \cdot \kappa_1 \gamma_j^h, \end{aligned}$$

$$\begin{aligned} (T_j^0)_N &= \left( -i k_0 \cdot (k_j + k_0)(c_0 \cdot k_0) \Gamma_j^{+1} - i |k_j + k_0| (c_0 \cdot k_0) \Gamma_j^{+1} \right. \\ &\quad \left. + |k_j + k_0| (\lambda_0 + i c_0 \cdot (k_j + k_0)) \Gamma_j^{+1} \right. \\ &\quad \left. - i k_0 \cdot (k_j - k_0)(c_0 \cdot k_0) \Gamma_j^{-1} - i |k_j - k_0| (c_0 \cdot k_0) \Gamma_j^{-1} \right. \\ &\quad \left. + |k_j - k_0| (\lambda_0 + i c_0 \cdot (k_j - k_0)) \Gamma_j^{-1} - 3\sigma |k_j|^2 \right. \\ &\quad \left. - (\gamma_j^{+1} + \gamma_j^{-1})(c_0 \cdot k_0)^2 + 2(1 + \sigma) + 2(k_j \cdot k_0) \omega(k_j) \right) \\ &\quad \times (c_0 \cdot k_0) + 2 \frac{(k_j \cdot k_0)(c_0 \cdot k_0) \omega(k_j) - |k_j| \omega(k_j)^2}{|k_j|}, \end{aligned}$$

$$\begin{aligned} T_j^{\pm 2} &= \left( -(c_0 \cdot k_0)^2 \gamma_j^{\pm 1} - \frac{2i \omega(k_j) k_j \cdot k_0 F_2}{|k_j|} \pm 2i \omega(k_j) F_2 \right. \\ &\quad \left. - \omega(k_j)^2 E_2 + 4i c_0 \cdot k_0 F_2 - i k_0 \cdot (k_j \pm k_0)(c_0 \cdot k_0) \Gamma_j^{\pm 1} \right. \\ &\quad \left. \pm i |k_j \pm k_0| (c_0 \cdot k_0) \Gamma_j^{\pm 1} + |k_j \pm k_0| (\lambda_0 + i c_0 \cdot (k_j \pm k_0)) \Gamma_j^{\pm 1} \right. \\ &\quad \left. + \frac{3}{2} \sigma k_2 \cdot (k_j \pm 2k_0) - (1 + \sigma) \right. \\ &\quad \left. - i k_j \cdot k_0 (\lambda_0 + i c_0 \cdot k_j)(c_0 \cdot k_0) \pm i (\lambda_0 + i c_0 \cdot k_j) \right. \\ &\quad \left. \times (c_0 \cdot k_0) + \frac{(k_j \cdot k_0)(c_0 \cdot k_0) \omega(k_j)}{|k_j|} \right. \\ &\quad \left. \mp \frac{|k_j|^2 (c_0 \cdot k_0) \omega(k_j) - |k_j| \omega(k_j)^2}{|k_j|} \right). \end{aligned}$$

These coefficients include contributions from  $\zeta_1$ ,  $u_1$ ,  $\eta_2$  and  $\Phi_2$ . The coefficients of the Fourier modes of  $\zeta_1$  and  $u_1$  are defined in (2.15). The coefficients of the second harmonics in  $\eta_2$  and  $\Phi_2$  appear in Eq. (2.2) and are referenced in the above formulae as

$$E_2 = \left( \frac{1 + \sigma}{1 - 2\sigma} \right) \quad \text{and} \quad F_2 = \left( \frac{3i\sigma \sqrt{1 + \sigma}}{1 - 2\sigma} \right).$$

Labeling the wave numbers so that  $k_1 = k_2 + 2k_0$ , the solvability conditions are

$$\begin{aligned} 2(\lambda_2 + i(c_0 - c_g(k_1)) \cdot \kappa_2) + \left( t_1^0 - \frac{\lambda_0 + i c_0 \cdot k_1}{1 + \sigma |k_1|^2} T_1^0 \right) \\ + \beta_{0,2} \left( t_2^{+2} - \frac{\lambda_0 + i c_0 \cdot k_1}{1 + \sigma |k_1|^2} T_2^{+2} \right) = 0, \end{aligned}$$

$$\begin{aligned} 2\beta_{0,2}(\lambda_2 + i(c_0 - c_g(k_2)) \cdot \kappa_2) + \left( t_1^{-2} - \frac{\lambda_0 + i c_0 \cdot k_2}{1 + \sigma |k_2|^2} T_1^{-2} \right) \\ + \beta_{0,2} \left( t_2^0 - \frac{\lambda_0 + i c_0 \cdot k_2}{1 + \sigma |k_2|^2} T_2^0 \right) = 0. \end{aligned}$$

In these solvability conditions appear the quartet interaction coefficients,  $P_{i,j}$ , which are the result of wavenumber  $k_j$  interacting with the Stokes wave to force equation (2.16) at wavenumber  $k_i$ , absent modulation. These coefficients are defined as

$$P_{1,1} = \left( \frac{\lambda_0 + i c_0 \cdot k_1}{1 + \sigma |k_1|^2} \tilde{T}_1^0 - \tilde{t}_1^0 \right),$$

$$P_{1,2} = \left( \frac{\lambda_0 + i c_0 \cdot k_1}{1 + \sigma |k_1|^2} T_2^{+2} - t_2^{+2} \right),$$

$$P_{2,1} = \left( \frac{\lambda_0 + i c_0 \cdot k_2}{1 + \sigma |k_2|^2} T_1^{-2} - t_1^{-2} \right),$$

$$P_{2,2} = \left( \frac{\lambda_0 + i c_0 \cdot k_2}{1 + \sigma |k_2|^2} \tilde{T}_2^0 - \tilde{t}_2^0 \right)$$

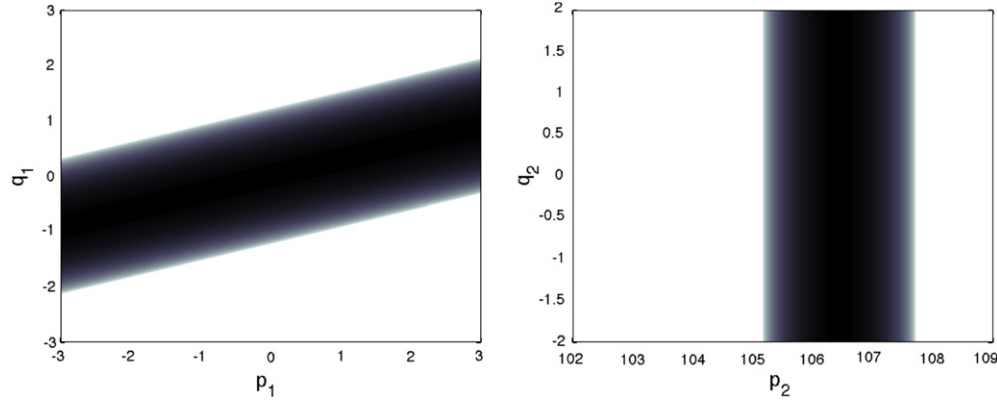


**Fig. 2.3.** The location of instabilities asymptotically near  $\kappa_0$  is approximated, on the left near a triad in the  $\kappa_1$  plane, on the right near a quartet in the  $\kappa_2$  plane. The triad resonance occurs at  $\kappa_0 \approx (0.2908, 0.1)$  and  $\sigma = 2.75$  when  $\epsilon = 0$ , and finite amplitude instabilities persist at this  $\kappa_0$  for  $\epsilon > 0$ . On the right, a quartet resonance occurs at  $\sigma = 0.24$  and  $\kappa_0 \approx (0.159, 0)$  at  $\epsilon = 0$ . In this case, finite amplitude instabilities do not occur at the resonant configuration; the origin in the  $\kappa_2$  plane is not within the band of instabilities.

where the terms with the tilde are evaluated at  $\kappa_1 = \kappa_2 = 0$ , i.e. absent modulational effects, so that the  $P_{i,j}$  match the definitions used in [13,28]. In terms of these quartet interaction coefficients, which are all pure imaginary, we can find the first non-zero correction to the free surface,

$$\lambda_2 = \frac{1}{4}(P_{2,2} + P_{1,1}) - i \left( c_0 - \frac{c_g(k_1) + c_g(k_2)}{2} \right) \cdot \kappa_2 \pm \frac{1}{4} \sqrt{(P_{2,2} - P_{1,1} + 2i(c_g(k_1) - c_g(k_2)) \cdot \kappa_2)^2 + 4P_{1,2}P_{2,1}}. \quad (2.17)$$

Since the  $P_{i,j}$  are pure imaginary,  $\lambda_2$  can have positive real part only if the product  $P_{1,2}P_{2,1}$  is positive. The strongest such instabilities will occur when

$$P_{1,1} - P_{2,2} = 2i(c_g(k_1) - c_g(k_2)) \cdot \kappa_2$$

which is generically a modulational instability, i.e. does not occur at  $\kappa_2 = 0$ . This is different from the triad case, where the largest instabilities are not modulational (the largest triad instabilities occur at  $\kappa_1 = 0$ ).

Whenever  $P_{1,2}P_{2,1} > 0$ , there are Bloch vectors causing modulational quartet instability satisfying

$$|2i(c_g(k_1) - c_g(k_2)) \cdot \kappa_2 - (P_{1,1} - P_{2,2})| < \sqrt{4P_{1,2}P_{2,1}}. \quad (2.18)$$

For deep water gravity waves, there is a quartet interaction at  $p_0 = 1/4$  which has  $P_{1,2} = P_{2,1} = 0$ . Eq. (2.18) predicts no instability in this case. Thus this asymptotic argument explains why there is no observed instability or loss of analyticity near  $(p, \epsilon) = (1/4, 0)$  in [13]. For gravity–capillary waves in deep water, there are quartets which lead to instability (see Fig. 2.3). The radii of convergence of the spectrum at Bloch parameters near one such quartet is compared to the prediction of (2.18) in the right panel of Fig. 2.2.

### 2.3. Higher order resonances

For finite amplitude spectra bifurcating from flat-state eigenvalue collisions of algebraic multiplicity two, the remaining cases (quintets, sextets, etc.) can be summarized as follows. For these higher order resonances, where  $|k_1 - k_2| > 2$ , with general  $\kappa_2$

$$\lambda_2 = -i(c_0 - c_g(k_1)) \cdot \kappa_2 + \frac{1}{2}P_{1,1},$$

$\beta_{0,2} = 0$  and the two eigenfunctions, are at leading order, decoupled. All later eigenvalue corrections  $\lambda_n$  are pure imaginary, and the eigenvalue collision does not cause instability. To have an

instability bifurcating from a quintet resonance a necessary, but not sufficient, condition is

$$2i(c_g(k_2) - c_g(k_1)) \cdot \kappa_2 = P_{1,1} - P_{2,2}. \quad (2.19)$$

Thus the Bloch parameter corrections  $\kappa_2$ , at which instabilities can occur, live on a line in the  $\kappa_2$  plane. Although the series is not computed here, we expect instability to be possible near quintet resonances for a line of  $\kappa_2$  and a band of the  $\kappa_3$  plane, near sextet resonances for a line in the  $\kappa_3$  plane and a band in the  $\kappa_4$  plane, etc. The locus of such instabilities will be at leading order at  $\kappa = \kappa_0 + \epsilon^2 \kappa_2$ , with  $\kappa_2$  from Eq. (2.19), whenever  $|k_1 - k_2| > 2$ . Thus although the sufficient conditions for the existence of such high order (and asymptotically small) instabilities are not reported, Eq. (2.19) predicts the locations of such instabilities. This intuition is consistent with the size and location of the instabilities computed in [20].

### 2.4. The Benjamin–Feir instability

The flat-state spectrum rarely has eigenvalue collisions of algebraic multiplicity larger than two, but one such collision occurs for all Bond numbers, and is responsible for the famous Benjamin–Feir instability. Note, although the multiplicity four eigenvalue collision occurs for all Bond numbers (and depths), the collision results in instability only for some. For example, deep-water waves in one space dimension are Benjamin–Feir stable for  $\sigma \in [2\sqrt{3}/3 - 1, \frac{1}{2}]$ , but still have a multiplicity four eigenvalue collision at zero amplitude. The location and size of the Benjamin–Feir instability can be predicted in this modulational framework. The Benjamin–Feir instability bifurcates from a flat-state eigenvalue collision at  $\lambda_0 = 0$ , of algebraic multiplicity 4 and geometric multiplicity 3; the eigenvectors are supported at three wave numbers,  $k_1 = k_0$ ,  $k_2 = -k_0$  and  $k_3 = 0$ . The flat-state eigenfunctions are

$$\begin{pmatrix} \zeta_0 \\ u_0 \end{pmatrix} = \begin{pmatrix} 1 \\ ic_0 \cdot k_0 \end{pmatrix} e^{ik_0 \cdot x} + \beta_{0,2} \begin{pmatrix} 1 \\ -ic_0 \cdot k_0 \end{pmatrix} e^{-ik_0 \cdot x} + \beta_{0,3} \begin{pmatrix} 0 \\ 1 \end{pmatrix}. \quad (2.20)$$

Eq. (2.10) now has solvability conditions at three frequencies, yielding

$$2(\lambda_1 + i(c_0 - c_g(k_1)) \cdot \kappa_1) = 0 \quad (2.21a)$$

$$2\beta_{0,2}(\lambda_1 + i(c_0 - c_g(k_2)) \cdot \kappa_1) = 0 \quad (2.21b)$$

$$\beta_{0,3}q_3^0 = 0. \quad (2.21c)$$

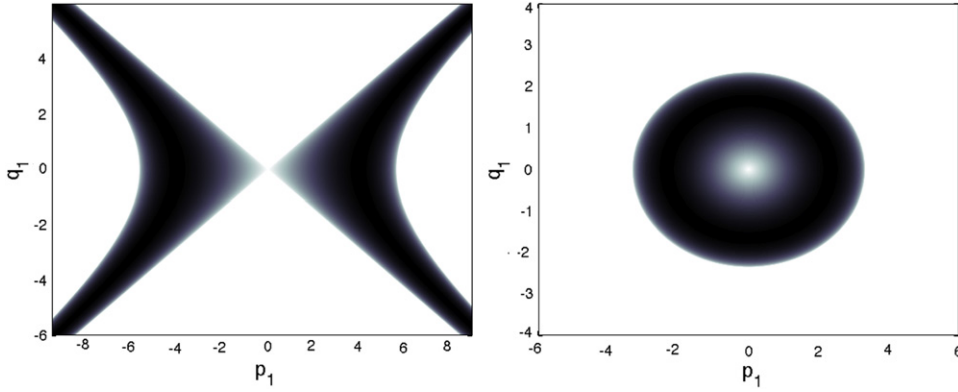


**Fig. 2.4.** The Benjamin–Feir instability region in the  $\kappa_1$  plane is shaded black (on the left with  $\sigma = 0$ , on the right with  $\sigma = 1$ ). This region is predicted by Eq. (2.24). The shape difference is due to a sign change in the Hessian of the linear dispersion relation, and is captured by Eq. (2.24).

Although the Benjamin–Feir wave numbers take part in multiple triad interactions, for example  $k_1 + k_3 = k_0$ ,  $k_3 - k_2 = k_0$ , these interactions are degenerate in multiple senses. The nonlinear interaction coefficients due to these interactions, the  $\tau_j$  of Section 2.1, are zero. The group velocities are also equal, so Eq. (2.21b) does not restrict the value of  $\beta_{0,2}$ . From Eq. (2.21c) we see that the mean flow term vanishes,  $\beta_{0,3} = 0$ . This is special to deep water;  $\beta_{0,3}$  is undetermined at this order of approximation in the finite-depth problem. The first correction to the flat-state eigenvalue is

$$\lambda_1 = -i(c_0 - c_g(k_1)) \cdot \kappa_1.$$

The solutions to (2.10) are identical to those of the previous section and are reported in Eq. (2.14), with the exception that since  $q_1^{-1} = q_2^{+1} = Q_1^{-1} = Q_2^{+1} = 0$ , the coefficients  $\gamma_1^{-1} = \gamma_2^{+1} = \Gamma_1^{-1} = \Gamma_2^{+1}$  are zero. Direct use of (2.15) would yield an indeterminate form. In the Benjamin–Feir case, Eq. (2.16) has three solvability conditions

$$2(\lambda_2 + i(c_0 - c_g(k_1)) \cdot \kappa_2) - i\kappa_1^T \cdot H(k_1) \cdot \kappa_1 - P_{1,1} - \beta_{0,2}P_{1,2} = 0 \quad (2.22a)$$

$$\beta_{0,2} (2(\lambda_2 + i(c_0 - c_g(k_2)) \cdot \kappa_2) - i\kappa_1^T \cdot H(k_2) \cdot \kappa_1) - P_{2,1} - \beta_{0,2}P_{2,2} = 0 \quad (2.22b)$$

$$\lambda_1 (\gamma_1^- + \beta_{0,2}\gamma_2^+) = 0. \quad (2.22c)$$

The  $P_{i,j}$  are the same quartet interaction coefficients reported in the previous section. The matrix  $H(k_j)$  is the Hessian of the dispersion relation  $\omega(k)$  evaluated at wavenumber  $k_j$ . The third equation in (2.22) provides no new information (since  $\lambda_1$  is known and  $\gamma_1^+ = \gamma_2^- = 0$ ). The first two equations in (2.22) determine the next eigenvalue correction given in Box 1.

In our choice of coordinates, the Stokes wave is oriented along the  $x$ -axis,  $k_0 = (1, 0)$ , and Eq. (2.23) can be simplified greatly. At  $k_0 = (1, 0)$ , the quartet interaction coefficients are

$$P_{1,1} = P_{1,2} = -P_{2,1} = -P_{2,2} = i \frac{2\sigma^2 + \sigma + 8}{2(1 - 2\sigma)\sqrt{1 + \sigma}}.$$

In addition,  $c_g(k_0) = c_g(-k_0)$ , and  $H(k_0) = -H(-k_0)$ , so that

$$H(k_0) = -H(-k_0) = \begin{pmatrix} \frac{3\sigma^2 + 6\sigma - 1}{4(1 + \sigma)^{3/2}} & 0 \\ 0 & \frac{1 + 3\sigma}{2(1 + \sigma)^{1/2}} \end{pmatrix},$$

$$\lambda_2 = -\frac{1}{2}i(c_0 - c_g(k_0)) \kappa_2 \pm \frac{1}{2}\sqrt{\kappa_1^T H(k_0) \kappa_1 (2iP_{1,1} - \kappa_1^T H(k_0) \kappa_1)}. \quad (2.24)$$

The region of instability, in the  $\kappa_1$  plane, based on the discriminant in Eq. (2.24) is plotted in Fig. 2.4. In the left panel of this figure is the famous Benjamin–Feir ‘X’, the instability region at  $\sigma = 0$ . In the right panel is the donut-shaped Benjamin–Feir instability region when  $\sigma = 1$ . The difference in shape is due to the change in sign of the entries of the Hessian: at  $\sigma = 0$  the Hessian has two opposite signed entries, at  $\sigma = 1$  it is of one sign. This sign change is the reason that capillary–gravity lump solitary waves exist near  $\sigma = 1$ , as in [47,48], but such waves do not exist in the absence of surface tension. This figure could also be computed in the context of the nonlinear Schrödinger equation (NLS), as in [36]; it is included here to show that the modulational spectrum includes the predictions of NLS.

If one considers perturbations whose principal modulation is in the longitudinal direction,  $\kappa_1 = (p_1, 0)$ , then instabilities exist in two adjacent intervals of Bloch parameter, between  $p_1 = 0$  and

$$p_1 = \pm \sqrt{\frac{4(2\sigma^2 + \sigma + 8)(1 + \sigma)}{(3\sigma^2 + 6\sigma - 1)(2\sigma - 1)}}. \quad (2.25)$$

Eq. (2.25) predicts the boundary across which the spectrum is not analytic in amplitude  $\epsilon$ , or frequency  $p$ , and is marked by the dashed line emanating from the origin in the left panel of Fig. 2.2.

### 3. Conclusion

The leading order asymptotics of the spectral data of traveling waves in infinite depth are derived using a modulational, multi-scale expansion. Formulae are also derived for the location of instabilities in frequency amplitude space. These formulae predict where the spectrum loses analyticity in amplitude, at locations which agree well with the numerical computations. Both transverse and longitudinal perturbations are considered. General collisions of two flat-state eigenvalues are considered, as is the Benjamin–Feir case, a special collision of four eigenvalues at the origin.

**Disclaimer:** This report was prepared as an account of work sponsored by an agency of the United States Government. Neither the United States Government nor any agency thereof, nor any of their employees, make any warranty, express or implied, or assume any legal liability or responsibility for the accuracy, completeness, or usefulness of any information, apparatus, product, or process disclosed, or represent that its use would not infringe privately owned rights. Reference herein to any specific commercial product, process, or service by trade name, trademark, manufacturer, or otherwise does not necessarily constitute or imply its endorsement, recommendation, or favoring by the United States Government or any agency thereof. The views and opinions of

$$2\lambda_2 = -i \left( c_0 - \frac{c_g(k_1) + c_g(k_2)}{2} \right) \kappa_2 + i \kappa_1^T \left( \frac{H(k_1) + H(k_2)}{2} \right) \kappa_1 + \frac{P_{1,1} + P_{2,2}}{2} \pm \frac{1}{2} \sqrt{(i(c_g(k_1) - c_g(k_2))\kappa_2 + i\kappa_1^T(H(k_1) - H(k_2))\kappa_1 + P_{1,1} - P_{2,2})^2 + 4P_{1,2}P_{2,1}} \quad (2.23)$$

### Box I.

authors expressed herein do not necessarily state or reflect those of the United States Government or any agency thereof.

### Acknowledgment

This work was partially supported by a grant from the Simons Foundation (#313852 to Benjamin Akers).

### References

- [1] T.B. Benjamin, J.E. Feir, The disintegration of wave trains on deep water, *J. Fluid Mech.* 27 (1967) 417–430.
- [2] O.M. Phillips, On the dynamics of unsteady gravity waves of finite amplitude. Part 1. The elementary interactions, *J. Fluid Mech.* 9 (1960) 193–217.
- [3] J.L. Hammack, D.M. Henderson, Resonant interactions among surface water waves, *Annu. Rev. Fluid Mech.* 25 (1993) 55–97.
- [4] A.D.D. Craik, *Wave Interactions and Fluid Flows*, Cambridge University Press, 1985.
- [5] D.J. Benney, Non-linear gravity wave interactions, *J. Fluid Mech.* 14 (04) (1962) 577–584.
- [6] R.S. MacKay, P.G. Saffman, Stability of water waves, *Proc. R. Soc. Lond. Ser. A* 406 (1986) 115–125.
- [7] J. McLean, Instabilities of finite-amplitude gravity waves on water of finite depth, *J. Fluid Mech.* 114 (1982) 331–341.
- [8] F. Dias, C. Kharif, Nonlinear gravity and gravity–capillary waves, *Annu. Rev. Fluid Mech.* 31 (1999) 301–346.
- [9] R. Tiron, W. Choi, Linear stability of finite-amplitude capillary waves on water of infinite depth, *J. Fluid Mech.* 696 (2012) 402–422.
- [10] M. Francius, C. Kharif, Three-dimensional instabilities of periodic gravity waves in shallow water, *J. Fluid Mech.* 561 (2006) 417–437.
- [11] B. Deconinck, O. Trichtchenko, Stability of periodic gravity waves in the presence of surface tension, *Eur. J. Mech. B Fluids* 46 (2014) 97–108.
- [12] D.P. Nicholls, F. Reitich, Stable, high-order computation of traveling water waves in three dimensions, *Eur. J. Mech. B Fluids* 25 (2006) 406–424.
- [13] B. Akers, D.P. Nicholls, Spectral stability of deep two-dimensional gravity water waves: repeated eigenvalues, *SIAM J. Appl. Math.* 72 (2012) 689–711.
- [14] K.B. Dysthe, Note on a modification to the nonlinear Schrodinger equation for application to deep water waves, *Proc. R. Soc. Lond. Ser. A* 369 (1979) 105–114.
- [15] A. Davey, K. Stewartson, On three-dimensional packets of surface waves, *Proc. R. Soc. A* 338 (1613) (1974) 101–110.
- [16] D.J. Benney, G.J. Roskes, Wave instabilities, *Stud. Appl. Math.* 48 (377) (1969) 377–385.
- [17] M. Stiassnie, L. Shemer, On modifications of the Zakharov equation for surface gravity waves, *J. Fluid Mech.* 143 (1984) 47–67.
- [18] A. Dixon, A stability analysis for interfacial waves using a Zakharov equation, *J. Fluid Mech.* 214 (1990) 185–210.
- [19] S.J. Hogan, The fourth-order evolution equation for deep-water gravity–capillary waves, *Proc. R. Soc. A* 402 (1823) (1985) 359–372.
- [20] B. Deconinck, K. Oliveras, The instability of periodic surface gravity waves, *J. Fluid Mech.* 675 (2011) 141–167.
- [21] A.J. Roberts, Highly nonlinear short-crested water waves, *J. Fluid Mech.* 135 (1983) 301–321.
- [22] A.J. Roberts, L.W. Schwartz, The calculation of nonlinear short-crested gravity waves, *Phys. Fluids* 26 (1983) 2388–2392.
- [23] T.R. Marchant, A.J. Roberts, Properties of short-crested waves in water of finite depth, *J. Aust. Math. Soc. Ser. B* 29 (1) (1987) 103–125.
- [24] L.W. Schwartz, Computer extension and analytic continuation of Stokes' expansion for gravity waves, *J. Fluid Mech.* 62 (3) (1974) 553–578.
- [25] D.P. Nicholls, Boundary perturbation methods for water waves, *GAMM-Mitt.* 30 (2007) 44–74.
- [26] D.P. Nicholls, Spectral data for traveling water waves: singularities and stability, *J. Fluid Mech.* 624 (2009) 339–360.
- [27] D.P. Nicholls, Spectral stability of traveling water waves: eigenvalue collision, singularities, and direct numerical simulation, *Physica D* 240 (4) (2011) 376–381.
- [28] B. Akers, D.P. Nicholls, Spectral stability of deep two-dimensional gravity capillary water waves, *Stud. Appl. Math.* 130 (2013) 81–107.
- [29] B. Akers, D.P. Nicholls, The spectrum of finite depth water waves, *Eur. J. Mech. B/Fluids* 46 (2014) 181–189.
- [30] D.P. Nicholls, Spectral stability of traveling water waves: analytic dependence of the spectrum, *J. Nonlinear Sci.* 17 (4) (2007) 369–397.
- [31] D.P. Nicholls, F. Reitich, On analyticity of traveling water waves, *Proc. R. Soc. Lond. Ser. A* 461 (2057) (2005) 1283–1309.
- [32] G.G. Stokes, On the theory of oscillatory waves, *Trans. Camb. Philos. Soc.* 8 (1847) 441–455.
- [33] R.J.C. Kamesvara, On ripples of finite amplitude, *Proc. Indian Ass. Cultiv. Sci.* 6 (1920) 175–193.
- [34] W.J. Harrison, The influence of viscosity and capillarity on waves of finite amplitude, *Proc. Lond. Math. Soc.* 7 (1909) 107–121.
- [35] J.R. Wilton, On ripples, *Phil. Mag.* 29 (1915) 173.
- [36] V.D. Djordjevic, L.G. Redekopp, On two dimensional packets of capillary–gravity waves, *J. Fluid Mech.* 79 (1977) 703–714.
- [37] T.J. Bridges, A. Mielke, A proof of the Benjamin–Feir instability, *Arch. Ration. Mech. Anal.* 133 (2) (1995) 145–198.
- [38] M. Oh, K. Zumbrun, Stability of periodic solutions of conservation laws with viscosity: analysis of the Evans function, *Arch. Ration. Mech. Anal.* 166 (2) (2003) 99–166.
- [39] J.C. Bronski, V.M. Hur, Modulational instability and variational structure, *Stud. Appl. Math.* 132 (4) (2014) 285–331.
- [40] V.M. Hur, M.A. Johnson, Modulational instability in the Whitham equation for water waves, 2013. ArXiv Preprint arXiv:1312.1579.
- [41] B. Akers, D.P. Nicholls, Traveling waves with gravity and surface tension, *SIAM J. Appl. Math.* 70 (2010) 2373–2389.
- [42] B. Akers, The generation of capillary–gravity solitary waves by a surface pressure forcing, *Math. Comput. Simulation* 82 (2012) 958–967.
- [43] M.S. Longuet-Higgins, The instabilities of gravity waves of finite amplitude in deep water. I. Superharmonics, *Proc. R. Soc. Lond. Ser. A* 360 (1703) (1978) 471–488.
- [44] M.S. Longuet-Higgins, The instabilities of gravity waves of finite amplitude in deep water. II. Subharmonics, *Proc. R. Soc. Lond. Ser. A* 360 (1703) (1978) 489–505.
- [45] B. Deconinck, J.N. Kutz, Computing spectra of linear operators using the Floquet–Fourier–Hill method, *J. Comput. Phys.* 219 (2006) 296–321.
- [46] B. Akers, P.A. Milewski, Model equations for gravity–capillary waves in deep water, *Stud. Appl. Math.* 121 (2008) 49–69.
- [47] B. Akers, P.A. Milewski, Dynamics of three dimensional gravity–capillary solitary waves in deep water, *SIAM J. Appl. Math.* 70 (2010) 2390–2408.
- [48] E.I. Parau, J.-M. Vanden-Broeck, M.J. Cooker, Nonlinear three-dimensional gravity–capillary solitary waves, *J. Fluid Mech.* 536 (2005) 99–105.